On Approximating the Translational Velocity of Vortex Rings

Michael Krieg
Department of Mechanical and Aerospace Engineering,
University of Florida,
Gainesville, FL 32611

Kamran Mohseni[1]
Department of Mechanical and Aerospace Engineering,
Department of Computer and Electrical Engineering,
Institute for Networked Autonomous Systems,
University of Florida, Gainesville, FL 32611
e-mail: mohseni@ufl.edu

A method is presented whereby the translational velocity of a vortex ring can be approximated from the total circulation, impulse, and kinetic energy of the vortex system. Assuming a uniform vorticity density, these bulk quantities define a unique stable vortex ring configuration, and the translational velocity can be inferred from this configuration and the system scaling. Here, the accuracy of this approximation is presented for vortex rings formed from starting jets, and the translational velocity is also characterized as it relates to the driving parameters. The translational velocity is well approximated for a wide range of experimentally generated vortex rings. It is observed that starting jets with a converging radial velocity create vortex rings with a significantly higher translational velocity. The converging radial velocity was observed to increase translational velocity by as much as 30% over parallel jet flows with identical volume flux and nozzle diameter, but the exact increase is specific to the nozzle arrangement and driving conditions. [DOI: 10.1115/1.4025287]

1 Introduction

Vortex rings are common coherent flow structures that appear in a wide range of fluid dynamic problems; a review of vortex rings is presented in Ref. [1]. One of the notable features of vortex rings is a period of steady translational velocity U_{tr} after the ring settles to a stable configuration. In practice vortex rings are generally created by ejecting an axisymmetric jet of fluid into a similarly dense resting fluid reservoir. The free end of the shear tube extending into the reservoir spirals up on itself rolling into a vortex ring. Jet flows created from cylinder-piston mechanisms enter the reservoir with nearly parallel streamlines, whereas jets ejected through a circular orifice in a flat plate contain a converging radial component of velocity. For both configurations, the piston velocity u_p is defined as the ratio of volume flux traveling through the nozzle to cross-sectional area $u_p = \forall/\pi R^2$. Here, $\forall$ is the volume flux passing through the nozzle and R is the nozzle radius. By this definition, the piston velocity is the average jet velocity passing through the orifice independent of the mechanism used to drive the flow.

The self-induced propagation velocity of vortex rings has been the subject of multiple studies. A formula for the translational velocity of a thin-cored vortex ring was given without proof by Lord Kelvin and later derived and expanded for the cases of uniform vorticity distribution in the vortex core by Fraenkel [2] and a hollow vortex core by Hicks [3]. Saffman [4] expanded this derivation to include any general vorticity distribution by use of a transformation inspired by Lamb [5]. The resulting translational velocity collapsed onto the velocities calculated by Fraenkel and Hicks when the core vorticity was set to a uniform and hollow distribution, respectively. Moffat and Fukumoto [6] expanded this derivation (which is accurate to the first order of the mean core radius ε) to be accurate to the third order of the mean core radius, ε, thus improving the solution for thick-cored vortex rings, even coming within 5% of the translational velocity of Hill's spherical vortex (a vortex ring of maximal thickness $\varepsilon = \sqrt{2}$ [7]). Applying a conservation of mass analysis and making basic assumptions about the nature of entrainment in the ring, Maxworthy related the decay rate of the translational velocity to the fluid viscosity [8,9], which showed a faster decay of translational velocity than predicted by Ref. [4] because the experimentally generated vortex rings had an appreciable thickness. The decay of vortex rings in confined spaces was related to circulation decay by Stewart et al. [10].

The velocity of arrays of vortex rings traveling in close succession are investigated, along with minimum separation distance by Krueger in Ref. [11], observing translational velocities close to half the piston velocity, similar to single vortex rings. Vortex rings created with inclined tube exits [12] do not show steady translational velocity, as the stopping and additional vortices become intertwined with the primary ring, creating much more dynamic behavior.

It should be noted that in the preceding investigations the translational velocity follows from an exact knowledge of the vorticity distribution inside the ring. However, this quantity is not often available and it cannot be easily calculated from the properties of the starting shear layer which is known for a given vortex generator. Determining the vorticity distribution of the resulting vortex ring from the parameters of the starting jet requires solving the evolution of the entire flow field, at which point the translational velocity does not need to be modeled and can be evaluated directly.

Considering the process of generating a steadily translating vortex ring from a starting jet as a statistical equilibrium process, Mohseni [13] has shown that all of the nonlinear Casimirs of motion $I_n = \int \omega^n dV$ will not be preserved at any resolvable scale during the formation process. Here ω is the local fluid vorticity. Thus, the flow will not have a memory of the higher moments of initial vorticity distribution. The only surviving invariants of motion will be the vortex energy, impulse, and the first Casimir of motion, namely the circulation $\Gamma = \int \omega dV$. The slightest amount of viscosity will violate conservation of the higher moment of vorticity; see Ref. [13]. This article is aimed at obtaining a formulation for translational velocity of a vortex ring based on the invariants of motion of its generating mechanism (since these invariants are preserved in the resulting vortex ring) instead of a formulation that requires direct knowledge of the vortex ring vorticity distribution. Using a variational analysis and equating the circulation, impulse, and energy of the vortex ring to that of a starting jet with an impulsive velocity program (u_p = constant) and uniform velocity profile, Mohseni and Gharib [14] arrived at the classic result that translational velocity is close to one-half the piston velocity. This analysis was extended to a wider range of mean core radii by Mohseni [15]. Additionally, the invariants of motion of starting jet flows with nonuniform axial velocity profiles, and nonzero radial velocity, where the 1D slug model provides a poor estimate, are derived in Ref. [16].

This paper presents a formulation for approximating the vortex ring translational velocity from the total circulation, impulse, and energy of the vortex ring. This analysis assumes that the vortex ring belongs to a family of known "standard" vortex rings, and the total jet quantities are used to identify the vortex ring configuration and resulting steady state translational velocity. Several vortex rings are created with fundamentally different translational velocities and core thicknesses to validate the accuracy of this approximation.

2 Velocity Approximation

The majority of vortex ring models are parameterized by the vortex ring toroidal radius l, translational velocity U_{tr}, mean core

[1]Corresponding author.

Contributed by the Fluids Engineering Division of ASME for publication in the Journal of Fluids Engineering. Manuscript received December 17, 2012; final manuscript received August 13, 2013; published online September 19, 2013. Assoc. Editor: Peter Vorobieff.

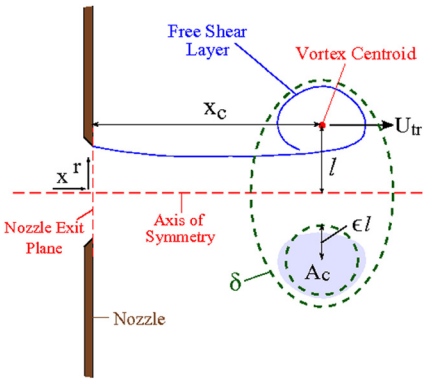

Fig. 1 Layout of a typical vortex ring created from a starting jet and coordinate system of the problem

radius ε, and vorticity density function Ω, as shown in Fig. 1. The mean core radius ε is a dimensionless parameter that describes the thickness of the vortex ring. For a vortex ring of core area A_c, the mean core radius is defined $\varepsilon \equiv [A_c/\pi l^2]^{1/2}$ and can range from $\varepsilon = 0$ for vortex filaments to $\varepsilon = \sqrt{2}$ for Hill's spherical vortex. The vorticity density function is defined $\Omega(x, r) \equiv \omega/r$; if the vorticity density is assumed to be constant within the core area, then there is a unique set of stable solutions for the vortex core boundary δ, which we refer to as the Norbury family of vortex rings [2,17–19], or sometimes called standard vortex rings. All vortex rings of this family can be collapsed onto a self-similar ring, and this set of rings varies purely as a function of the mean core radius ε. The circulation, impulse, and energy of Norbury vortices are normalized by the toroidal radius, mean core radius, and vorticity density:

$$\Gamma_c = \left(\Omega\varepsilon^2 l^2\right) l \Gamma_N \tag{1a}$$

$$I_c = \rho\left(\Omega\varepsilon^2 l^2\right) l^3 I_N \tag{1b}$$

$$E_c = \rho\left(\Omega\varepsilon^2 l^2\right)^2 l^3 E_N \tag{1c}$$

Here the subscript c refers to the values of the vortex ring and the subscript N refers to the normalized quantities as reported by Norbury [17]. Instead of scaling by the characteristic ring parameters the ring energy can be nondimensionalized by the other two bulk flow quantities so that the dimensionless energy becomes $\alpha = E_c/\left(I_c^{1/2}\Gamma_c^{3/2}\right)$, as was done in Refs. [13,14,20,21]. Note that this normalization eliminates the geometric scaling terms of Eq. (1) so that for vortex rings in the Norbury family $\alpha = E_N/(I_N^{1/2}\Gamma_N^{3/2})$, which is purely a function of ε.

Similarly, if the translational velocity of the vortex ring U_{tr} is known then the circulation can also be made dimensionless $\beta = \Gamma_c/(I_c^{1/3}U_{tr}^{2/3})$ as was done in Refs. [13,14]. Again the dimensionless circulation is purely a function of mean core radius for standard vortex rings, $\beta = \Gamma_N/(I_N^{1/3}W^{2/3})$, where W is the normalized translational velocity of the vortex ring defined in Ref. [17], $U_{tr} = (\Omega\varepsilon^2 l^2)W$.

Therefore, if the circulation, impulse, and energy of the vortex ring are all known, then the mean core radius can be interpolated from the dimensionless energy α. Additionally the translational velocity can then be determined from the dimensionless circulation corresponding to that mean core radius:

$$U_{tr} = \Gamma_c^{3/2}/\left(I_c^{1/2}\beta^{3/2}(\varepsilon)\right) \tag{2}$$

For reference the dimensionless energy and circulation, as determined in Ref. [17], are depicted in Fig. 2(*a*) with respect to mean core radius. Fortunately, the dimensionless energy and circulation have a relationship that eliminates the need to interpolate ε. Figure 2(*b*) shows the inverse of the nondimensional energy $1/\alpha$, plotted with respect to the corresponding nondimensional circulation taken to the power of 3/2 ($\beta^{3/2}$). It can be seen in this figure that the quantities have a nearly linear proportionality, which is demonstrated by the line fitted to the form $\beta^{3/2} = c_1 + c_2/\alpha$, with $c_1 = 1.13$ and $c_2 = 0.52$. This allows the translational velocity of the vortex ring to be written in terms of the bulk quantities alone:

$$U_{tr} = \frac{\Gamma_c^{3/2} E_c}{c_1 I_c^{1/2} E_c + c_2 I_c \Gamma_c^{3/2}} \tag{3}$$

This is a useful conclusion because the total circulation, impulse, and energy can be determined in starting jet flows from the jet velocity profile [22].

Next we experimentally evaluate the validity of this approximation for translational velocity for experimentally generated vortex rings. As was mentioned previously, the Norbury family of vortex rings is derived assuming that the vorticity density function $\Omega = \omega/r$ is constant over the cross-sectional area of the vortex core. In actuality, the vorticity distribution in stable vortex rings is not proportional to the distance from the axis of symmetry but exhibits an almost bell shape vorticity distribution centered about

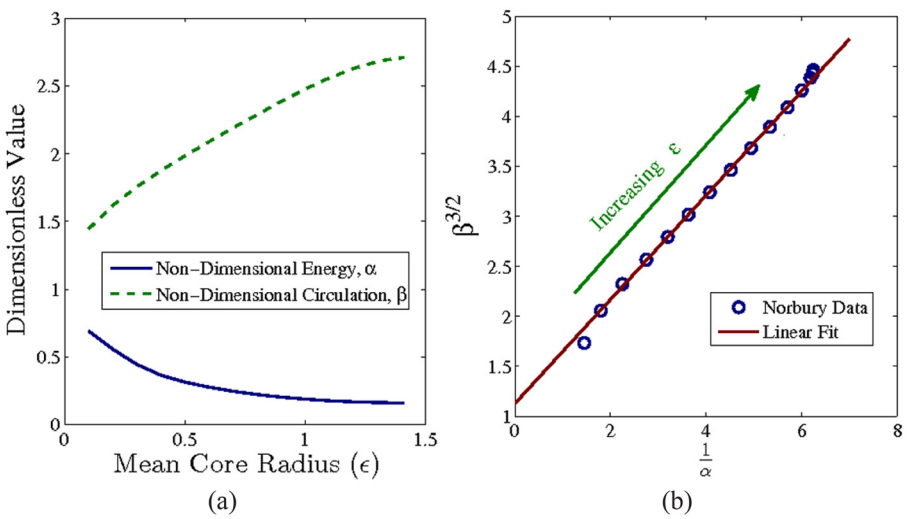

Fig. 2 Dimensionless energy and circulation for the Norbury family of vortices [17] are shown (*a*) with respect to mean core radius ε and (*b*) with respect to each other

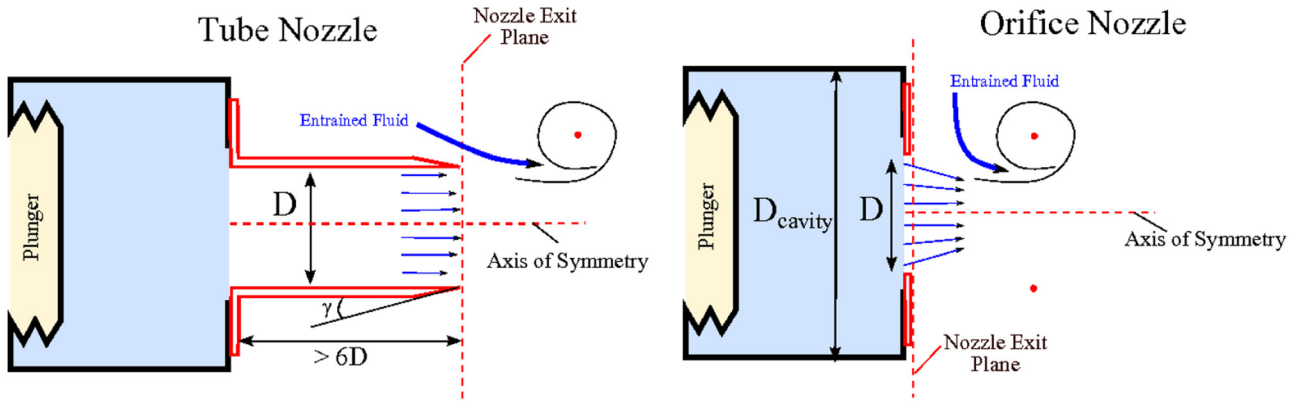

Fig. 3 Conceptual diagram of the layout of different nozzles used to generate various jet flows for this experiment

Table 1 Summary of experimental trials used in this investigation. Piston velocity and Re range listed for all trials in each case. Nondimensional energy, velocity ratio, and approximation accuracy are all calculated after the jet has settled on a stable configuration.

Case	Nozzle	radius (cm)	$\frac{L}{D}$	# trials	u_p (cm/s)	Re/1000	α (Std. dev.)	$\frac{U_{tr}}{u_p}$ (Std. dev.)	η (%) (Std. dev.)
1	Tube	1.3	2.4	5	5–13	1.3–10	0.38 (±0.03)	0.47 (±0.02)	4.1 (±3.3)
2	Tube	0.91	6.9	4	6.5–11	5.5–15.6	0.24 (±0.01)	0.60 (±0.05)	4.5 (±2.0)
3	Orifice	1.3	2.4	5	6.5–13	4–10.5	0.33 (±0.03)	0.77 (±0.03)	1.1 (±0.6)
4	Orifice	0.93	6.8	3	5.5–9	4–10.5	0.31 (±0.03)	0.78 (±0.02)	2.1 (±2.5)

the vortex center of vorticity [23–25]; the exact vorticity distribution is modeled in great detail by Fukumoto and Kaplanski [26]. However, it should be noted that the analysis of Saffman [4] for thin-cored rings showed no change in translational velocity for different vorticity distributions, provided that the vorticity density function is symmetric about the centroid. Therefore, this manuscript will also loosely demonstrate whether a similar invariance exists for thick vortex rings as well.

3 Vortex Generator

The fluid actuator used to create the vortex rings in this investigation consists of a sealed off canister submerged in a fluid reservoir. The vortex generator has an internal cavity with a moving plunger to move fluid in or out of the cavity; see Fig. 3. The plunger is a semiflexible accordion style bellows that expands axially but maintains a constant diameter. The expansion is driven by a mechanical system with an ability to create any desired deflection program. The cavity is attached to both tube and orifice nozzles in order to create both parallel and converging jets. The different nozzle arrangements are illustrated in Fig. 3.

When a jet is expelled through the orifice nozzle, some of the fluid inside the cavity must converge to the center in order to pass through the nozzle, and these converging streamlines persist downstream resulting in a converging radial velocity. The tube nozzle is a long tube connected to the end of the cavity. The tube is sufficiently long, $>6D$, to ensure a parallel jet flow in the tube prior to ejection. The outside of the tube is tapered at the exit with an angle γ, as shown in Fig. 3. The tube nozzles used in this investigation have a taper angle of $\gamma \approx 11$ deg.

Unlike cylinder-piston mechanisms that have a constant diameter and adjust stroke ratio L/D, by extending the piston displacement, this assembly expels a uniform jet volume and uses nozzles of varying diameter to change the jet stroke ratio. As is summarized in Table 1, large stroke ratio jets are created with tube and orifice nozzles of radius $R = 0.93$ cm and small stroke ratio jets from nozzles with radius $R = 1.3$ cm.

4 Experimental Setup

The experimental setup for this research is comprised of a tank that houses a large fluid reservoir, a high-speed flow visualization and filming system, and a data acquisition assembly that controls and records motor position and synchronizes filming and jet actuation. The vortex generator is sealed within a transparent canister that is submerged fully within the fluid in the testing tank. An illustration of this setup is provided in Fig. 4 along with a picture of the actual setup.

The water tank is 2.4 m tall, and 1 by 1.3 m in cross section and houses 2.65 kl of water. The tank is made out of acrylic to allow for visual access from all angles (including the bottom of the tank) and is supported by an outer steel skeleton. At the top of the tank is a mounting structure that holds the vortex generator in place. The flow visualization is performed using a high-speed camera and illumination apparatus. As depicted in Fig. 4(*a*) a 2D cross section of the flow is illuminated with a laser sheet. The laser sheet is generated by a 1 W 532 nm laser (Aixis GAM 1000B) expanded through a cylindrical lens within the tank, and is $\approx$1 mm thick. The illuminated cross section of the flow is recorded at 150–250 frames per second depending on the piston velocity. The camera used is a monochrome Phantom v210.

5 Digital Particle Image Velocimetry (DPIV) Analysis Description

The high-speed video of the jet flow is analyzed using a commercial software, with DPIV algorithms similar to those described in Refs. [27,28] to determine a velocity field $\vec{u} = [u, v]^T$ in the illuminated cross section of the jet flow. Frames (1280×800 pixel resolution), were divided into 32×32 pixel interrogation windows (with 50% overlap). Depending on exact nozzle diameter and optical zoom, the total DPIV velocity field domain ranged from 3.83×6.12 diameters to 5.22×8.35 diameters, with the long dimension of the image aligned with the axis of symmetry, resulting in relative resolutions in the range 10–12 grid-points per diameter. Strict care was taken to ensure that the laser sheet

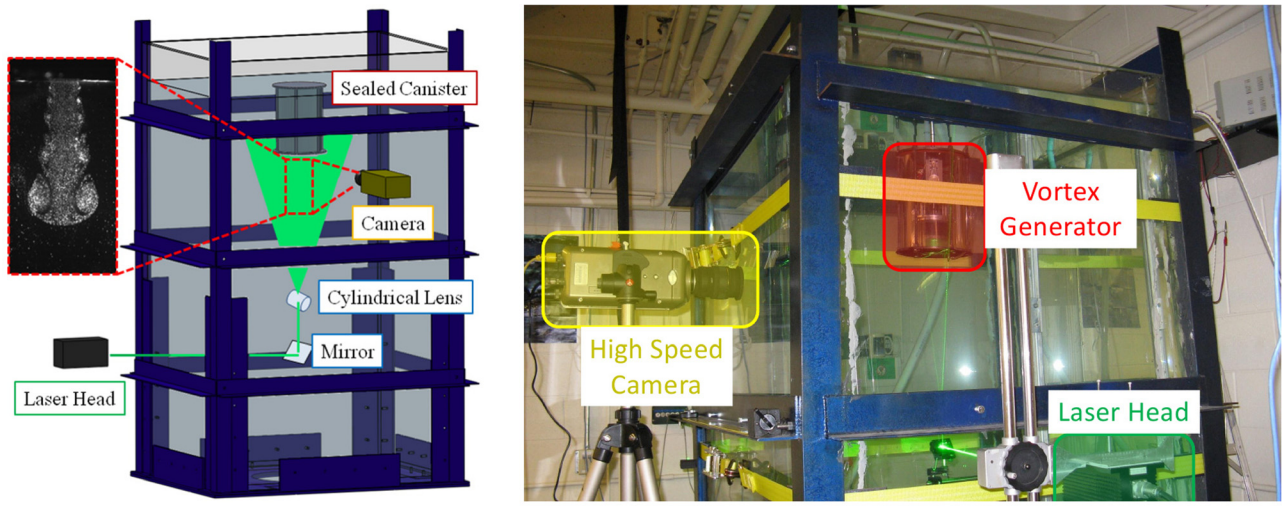

(a) (b)

Fig. 4 Testing environment; (*a*) schematic diagram and (*b*) actual layout. Tank is approximately 1 m × 1.3 m × 2.4 m.

bisected the flow through the jet axis of symmetry so that the filmed jet flow corresponds to axisymmetric flow.

The boundary of the vortex ring core δ is determined from the vorticity field as an isovorticity contour at some small threshold value ω_ε, which is above the background noise level. It should be noted that the isovorticity contour corresponding to the vortex boundary often includes multiple rings in the trailing wake for large stroke ratio jets. Therefore, the leading vortex ring core boundary is determined as the closed isovorticity contour enclosing the peak vorticity. Defining the core area A_c as the region encompassed by the core boundary δ and assuming the flow to be axisymmetric with no swirl, the circulation, impulse, and energy of the leading vortex ring can be determined from the vorticity and velocity fields [29,30].

$$\begin{aligned} \Gamma_c &= \int_{A_c} \omega dr dx, \\ I_c &= \pi \int_{A_c} \omega r^2 dr dx, \\ E_c &= \pi \int_{A_c} \left(u^2 + v^2\right) r dr dx \end{aligned} \tag{4}$$

Of course the center of vorticity of the vortex ring, whose motion is used to calculate the translational velocity of experimentally generated rings, is not necessarily at the same location as the peak vorticity value. The definition of the center of vorticity is given in Refs. [5,31] in terms of vorticity integral quantities. Restricting the integrals to the vortex core area A_c allows the vortex centroid to be determined:

$$l^2 = \frac{\int_{A_c} \omega_\phi r^2 dr dx}{\int_{A_c} \omega_\phi dr dx}, x_c = \frac{\int_{A_c} \omega_\phi r^2 x dr dx}{\int_{A_c} \omega_\phi r^2 dr dx} \tag{5}$$

Here, l and x_c are the radial and axial positions of the center of vorticity as depicted in Fig. 1.

Now the translational velocity and invariants of motion of experimentally generated vortex rings can be determined from DPIV data.

6 Results

The vortex generator of this investigation was used to create vortex rings from both parallel and converging starting jets with both high and low stroke ratios. Jets with low stroke ratio roll into a single vortex ring, whereas jets with higher stroke ratio produce a leading vortex ring and trailing wake, as was observed by Gharib et al. [21].

The jet flows examined in this study have a nearly impulsive velocity program. This means that the piston velocity of the jet rapidly accelerates at the onset of flow then maintains a nearly constant value for the remainder of pulsation. The resulting jets are filmed in cross section and the video analyzed as described previously to recover a history of circulation, impulse, and energy of the leading vortex ring, as well as the motion of the center of vorticity.

The experimental trials are summarized in Table 1. Each case listed (set of nozzle type and nozzle radius) has a range of trials with different piston velocities, which are listed in the table, but for each trial the piston velocity was held relatively constant. We define the accuracy of the velocity approximation as, $\eta = \left|U_{\text{tr-approximate}} - U_{tr-PIV}\right| / U_{tr-PIV}$, which is also listed in the table for the different cases. Values for U_{tr}/u_p, η, and α are calculated a sufficient amount of time after pulsation when the vortex ring has settled. The values are then averaged for all trials, which are reported along with the standard deviation. Table 1 also reports the jet Reynolds numbers calculated as $\text{Re} = \Gamma_c/\nu$, and the vortex ring circulation is averaged over the same period of time as U_{tr}/u_p, η, and α.

Lord Kelvin stated that the motion of a vortex system will minimize the energy Hamiltonian of the system, under area preserving isovortical perturbations [32,33]. This equates the translational velocity, a Lagrange multiplier of impulse in the energy Hamiltonian, to the ratio $U_{tr} = \delta E/\delta I$. Using the 1D slug model approximation ($u(r) = u_p$, $v(r) = 0$) to calculate total circulation, impulse, and energy created in the jet and equating the vortex system to the Norbury family of vortex rings, Mohseni et al. [14,15] derived the translational velocity in terms of piston velocity from Kelvin's variational theorem. This analysis showed that the translational velocity will be approximately half the piston velocity, $U_{tr} \approx 1/2 u_p$. This relationship has been well documented for parallel starting jets; however, the 1D slug model is demonstrated to be a poor prediction of nonparallel starting jets [22] so the relationship between piston velocity and translational velocity is likely very different.

Equation (3) gives an approximation for the translational velocity of a steady vortex ring in the Norbury family with specified circulation, impulse, and energy. The actual translational velocity of several vortex rings was determined from the motion of the center of vorticity of the leading vortex ring. The measured translational velocity is shown in Fig. 5, as well as the translational

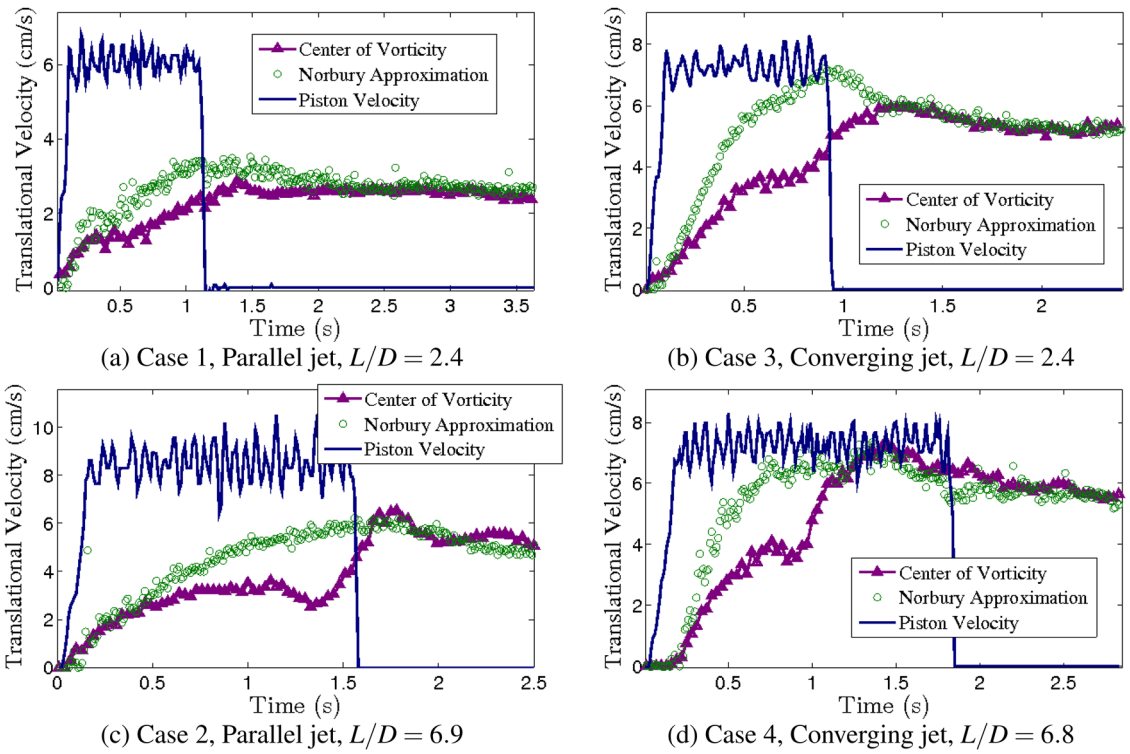

Fig. 5 Vortex ring translational velocity and piston velocity versus formation time, t^*, for (*a*) case 1, (*b*) case 3, (*c*) case 2, and (*d*) case 4, as summarized in Table 1

velocity as predicted by Eq. (3) using circulation, impulse, and energy of the primary vortex ring measured from DPIV data, Eq. (4). Figure 5 also shows the piston velocity over the same time period as a reference velocity.

Figures 5(*a*) and 5(*b*) (corresponding to cases 1 and 3 in Table 1) show that the translational velocity of steady vortex rings created from jets with a low stroke ratio is well predicted by Eq. (3), but the vortex ring only settles upon a stable configuration after the formation dynamics have subsided. During the period of substantial vortex ring growth, the actual vortex ring translational velocity is not predicted accurately. In general low stroke ratio jets create thin-cored vortex rings, as evidenced by the low nondimensional energy α of case 1 as reported in Table 1; case 3 creates a thicker ring because of the increased circulation flux associated with the converging radial velocity. Therefore, Eq. (3) can be considered valid for thin vortex rings, despite the poorly represented vorticity density function.

The jets expelled with a higher stroke ratio, Figs. 5(*c*) and 5(*d*) (cases 2 and 4), experience a much more energetic/dynamic pinch-off that results in oscillations in both U_{tr} and l as the primary vortex ring settles upon a stable configuration due to the interaction of the leading vortex ring with the trailing jet. Eventually these vortex rings stabilize and translational velocity closely approaches the predicted velocity of Eq. (3), but the vortex ring does not acquire a stable configuration until well after pinch-off, when there is a large enough distance between the leading vortex ring and the trailing wake. This demonstrates that the propagation velocity is very sensitive to the formation dynamics. Since high stroke ratio jets create thicker vortex rings (see Table 1) Eq. (3) can also be considered an accurate approximation for thick vortex rings, suggesting that thick rings also have similar translational velocities for different vorticity distributions, provided that those distributions are symmetric.

It can also be seen that despite the similar piston velocities the vortex rings formed from the converging jets have significantly larger translational velocities. After settling on a stable configuration, vortex rings created from the parallel starting jets have an average translational velocity close to half the piston velocity, $47 \pm 2\%$ for low stroke ratio (case 1) and $60 \pm 5\%$ for large stroke ratio (case 2), whereas the converging jet vortex rings have average translational velocities that are $77 \pm 3\%$ of the piston velocity for low stroke ratio (case 3) and $78 \pm 2\%$ of the piston velocity for large stroke ratio (case 4). This could help explain a large variation in reported vortex ring translational velocities with the same piston velocity.

7 Conclusion

This study provides a heuristic method for approximating the translational velocity of a vortex ring from the total circulation, impulse, and energy of the ring. The technique essentially equates the vortex ring to a member of a known family of stable vortex rings, and the translational velocity is inferred from the known configuration.

Multiple vortex rings were created experimentally and analyzed using standard DPIV techniques. The method proposed here predicted the translational velocity of the ring very well after the ring had settled on a stable configuration, for all cases, including vortex rings created from converging starting jets where standard 1D slug approximations fall short. Additionally, this approximation is observed to be equally accurate when predicting translational velocity of thin core versus thick core vortex rings. During the initial formation stages, the ring has not settled on a stable configuration and will not achieve the same translational velocity of a stable ring with the same circulation, impulse, and energy.

Acknowledgment

This work is supported by a grant from the Office of Naval Research.

Nomenclature

$A_C =$ vortex ring core area
$E =$ energy
$I =$ impulse
$l =$ vortex ring toroidal radius

$R =$ nozzle radius
$U_{tr} =$ vortex ring translational velocity
$u_p =$ piston velocity
$\alpha =$ nondimensional energy of the vortex ring
$\beta =$ nondimensional circulation of the vortex ring
$\varepsilon =$ vortex ring mean core radius
$\Gamma =$ circulation
$\Omega =$ vorticity density (distribution) function

References

[1] Shariff, K., and Leonard, A., 1992, "Vortex Rings," Ann. Rev. Fluid Mech., **34**, pp. 235–279.
[2] Fraenkel, L., 1970, "On Steady Vortex Rings of Small Cross-Section in an Ideal Fluid," Proc. R. Soc. Lond., **316**, pp. 29–62.
[3] Hicks, W. M., 1884, "On the Steady Motion and Small Vibrations of a Hollow Vortex," Phil. Trans. A, **175**, pp. 161–195.
[4] Saffman, P. G., 1970, "The Velocity of Viscous Vortex Rings," Stud. Appl. Math., **49**(4), pp. 371–379.
[5] Lamb, H., 1945, *Hydrodynamics*, Dover, New York.
[6] Moffatt, H., and Fukumoto, Y., 2000, "Motion and Expansion of a Viscous Vortex Ring. Part 1. A Higher-Order Asymptotic Formula for the Velocity," J. Fluid Mech., **417**, pp. 1–45.
[7] Hill, M. J. M., 1894, "On a Spherical Vortex," Phil. Trans. Roy. Soc. A, **185**, pp. 213–245.
[8] Maxworthy, T., 1972, "The Structure and Stability of Vortex Rings," J. Fluid Mech., **51**(1), pp. 15–32.
[9] Maxworthy, T., 1977, "Some Experimental Studies of Vortex Rings," J. Fluid Mech., **80**, pp. 465–495.
[10] Stewart, K. C., Niebel, C. L., Jung, S., and Vlachos, P. P., 2012, "The Decay of Confined Vortex Rings," Exp. Fluids, **53**, pp. 163–171.
[11] Krueger, P. S., 2009, "Vortex Ring Velocity and Minimum Separation in an Infinite Train of Vortex Rings Generated by a Fully Pulsed Jet," Theor. Comput. Fluid Dyn., **24**, pp. 291–297.
[12] Troolin, D. R., and Longmire, E. K., 2010, "Volumetric Velocity Measurements of Vortex Rings From Inclined Exits," Exp. Fluids, **48**, pp. 409–420.
[13] Mohseni, K., 2001, "Statistical Equilibrium Theory of Axisymmetric Flows: Kelvin's Variational Principle and an Explanation for the Vortex Ring Pinch-Off Process," Phys. Fluids, **13**(7), pp. 1924–1931.
[14] Mohseni, K., and Gharib, M., 1998, "A Model for Universal Time Scale of Vortex Ring Formation," Phys. Fluids, **10**(10), pp. 2436–2438.
[15] Mohseni, K., 2006, "A Formulation for Calculating the Translational Velocity of a Vortex Ring or Pair". Bioinspir. Biomimet., **1**, pp. S57–S64.
[16] Krieg, M., and Mohseni, K., 2013, "Modelling Circulation, Impulse and Kinetic Energy of Starting Jets With Non-Zero Radial Velocity," J. Fluid Mech., **719**, pp. 488–526.
[17] Norbury, J., 1973, "A Family of Steady Vortex Rings," J. Fluid Mech., **57**(3), pp. 417–431.
[18] Norbury, J., 1972, "A Steady Vortex Ring Close to Hill's Spherical Vortex," Proc. Camb. Phil. Soc., **72**, pp. 253–284.
[19] Fraenkel, L., 1972, "Examples of Steady Vortex Rings of Small Cross-Section in an Ideal Fluid," J. Fluid Mech., **51**(1), pp. 119–135.
[20] Friedman, A., and Turkington, B., 1981, "Vortex Rings: Existence and Asymptotic Estimates," Trans. Am. Math. Soc., **268**, pp. 1–37.
[21] Gharib, M., Rambod, E., and Shariff, K., 1998, "A Universal Time Scale for Vortex Ring Formation," J. Fluid Mech., **360**, pp. 121–140.
[22] Krieg, M., and Mohseni, K., 2012, "Modelling Circulation, Impulse, and Kinetic Energy of Starting Jets With Non-Zero Radial Velocity," J. Fluid Mech., **719**, pp. 488–526.
[23] Glezer, A., and Coles, D., 1990, "An Experimental Study of Turbulent Vortex Rings," J. Fluid Mech., **211**, pp. 243–283.
[24] Weigand, A., and Gharib, M., 1997, "On the Evolution of Laminar Vortex Rings," Exp. Fluids, **22**, pp. 447–457.
[25] Cater, J. E., Soria, J., and Lim, T. T., 2004, "The Interaction of the Piston Vortex With a Piston-Generated Vortex Ring," J. Fluid Mech., **499**, pp. 327–343.
[26] Fukumoto, Y., and Kaplanski, F., 2008, "Global Time Evolution of an Axisymmetric Vortex Ring at Low Reynolds Numbers," Phys. Fluids, **20**(5), p. 053103.
[27] Willert, C., and Gharib, M., 1991, "Digital Particle Image Velocimetry," Exp. Fluids, **10**, pp. 181–193.
[28] Raffel, M., Willert, C. E., and Kompenhans, J., 1998, *Particle Image Velocimetry*, Springer, Heidelberg/New York.
[29] Saffman, P., 1992, *Vortex Dynamics*, Cambridge University Press, Cambridge, UK.
[30] Lim, T., and Nickels, T., 1995, "Vortex Rings," *Fluid Vortices*, S. I. Green, ed. Kluwer Academic Publishers, Dordrecht, The Netherlands.
[31] Marshall, J. S., 2001, *Inviscid Incompressible Flow*, Wiley, New York, pp. 260–292.
[32] Kelvin, L., 1867, "The Translatory Velocity of a Circular Vortex Ring," Phil. Mag., **4**, pp. 511–512.
[33] Kelvin, L., 1910, *Mathematical and Physical Papers*, Vol. IV, Cambridge University Press, Cambridge, UK.